17th World Conference on Earthquake Engineering, 17WCEE
Sendai, Japan - September 13th to 18th 2020

SEISMIC PERFORMANCE OF PRECAST POST-TENSIONED SEGMENTAL COLUMNS USING INCREMENTAL DYNAMIC ANALYSIS

E. Ahmadi[(1)], M.M. Kashani[(2)]

[(1)] *Research Associate, University of Southampton, e.ahmadi@soton.ac.uk*
[(2)] *Associate Professor, University of Southampton, mehdi.kashani@soton.ac.uk*

Abstract

Precast post-tensioned segmental (PPS) columns lower vulnerability of bridges because of natural hinges and rocking motion of the segments. The use of the PPS columns in bridge construction is increasing as high-quality segments are constructed offsite, and are rapidly put together onsite. Hence, the seismic performance assessment of the PPS columns is necessary to expand and improve seismic application of these columns. Therefore, this study investigates seismic behavior of the PPS columns using incremental dynamic analysis (IDA). To this end, an experimentally validated Finite Element model in OpenSees program is adopted to analyze three PPS columns with different aspect ratios. The IDA results show that the maximum seismic responses of the columns occur at their base, and also the aspect ratio of the column plays a crucial role in seismic performance assessment of the PPS columns. It is also found from fragility curves that squat columns are more prone to seismic collapse compared to slender columns.

Keywords: precast post-tensioned segmental columns, accelerated bridge construction, incremental dynamic analysis, far-fault ground motions, seismic performance assessment

1. Introduction

The monolithically constructed cast-in-place (CIP) reinforced concrete (RC) columns are highly prone to concrete cracks, yielding and buckling of reinforcing bars subject to lateral extreme seismic loadings. This is mostly occurring at the base of the columns where the largest shear force and bending moment coexist. Hence, the precast post-tensioned segmental (PPS) columns are an excellent alternative to achieve a more resilient bridge structure (i.e. low damage probability and longer service life). Offsite manufacturing of the segments of the PPS columns results in a higher concrete quality, shorter construction time, and ease of construction. Additionally, the rocking mechanism of the segments avoids large concrete cracks.

Many experimental works have studied structural behavior of the PPS columns mostly under quasi-static cyclic loading and rarely dynamic excitations. Hewes [1] studied structural performance of the PPS columns with different aspect ratios through a number of cyclic tests. It was found that the PPS columns have effective resistance against seismic loading while having low energy-dissipating capacity. To enhance energy-dissipating capacity of the PPS columns, different methods were suggested throughout quasi-static and cyclic testing protocols ([2, 3]). In rare cases, shake table tests including actual ground motions as base excitations were conducted to investigate structural performance of the PPS columns enhanced with external attachments for energy dissipation ([4, 5]). In a series of different studies, shake table tests using sweep sine base excitations were carried out on small-scale segmental columns with layers of high-damping materials placed between their segments ([6, 7, 8, 9]). In addition to the experimental works, many numerical studies have been also performed on the PPS columns. 3D continuum finite element (FE) models [10] and fiber-based FE models ([11],[12]]) were used to determine dynamic demands of the PPS columns. The continuum FE models are able to realistically simulate local damages at the compression zones of the contact surfaces between the segments. However, these models lack calculation efficiency particularly in case of nonlinear time history analysis where a large number of actual ground motions are intended to be used. Unlike the continuum FE models, the fibre-based FE models are computationally efficient. However, they cannot simulate the contact surface between segments of the PPS columns. Cai et al. [13] numerically explored key factors influencing residual drifts of the PPS columns equipped with energy-dissipating bars focusing on cyclic behavior only. Most of these numerical models were used to validate experimental results focusing only on quasi-static and cyclic behavior of the PPS columns. In a new study, Ahmadi and Kashani [14] developed a computationally efficient FE model for the PPS columns in OpenSees program [15] where the segments were modelled as elastic blocks and the contact surfaces were simulated using a number of zero-tension elastic springs. The model was experimentally validated throughout a number of quasi-static and shake table tests. As the above literature survey demonstrated, even though quasi-static and cyclic behavior of the PPS columns have received much attention, their seismic performance subject to an ensemble of actual ground motion records yet to be quantified using advanced nonlinear dynamic analyses. Therefore, this study focuses on seismic behavior of the PPS columns using Incremental Dynamic Analysis (IDA) tool for the first time [16]. To reach this goal, an experimentally-validated and highly efficient numerical model in OpenSees program [15] is used to analyze three PPS columns with different aspect ratios. Then, the IDA and fragility curves of the PPS columns are generated subject to 44 far-fault ground motion records.

2. The Studied PPS Columns

Three PPS columns of different aspect ratio are used in this work. As shown in Figure 1, the PPS columns are composed of n precast concrete segments of width B and total height of H, and support a bridge deck on top of the segments. The axial load from the top deck is defined as a ratio of the axial capacity of the concrete section, N/(fcAg), where N is the axial load, fc is the concrete compressive strength, and Ag is the gross cross section area of each column. The segments are tightened together by a post-tensioning stainless steel tendon, fixed at the base and at the top of the column. The tendon provides a self-centering mechanism in the column under lateral loading scenarios. Table 1 summarizes the properties of the columns used in this study. The columns consist of 2, 4, and 8 square segments with heights of 1, 2, and 3 m, which represent squat, slender, and very slender PPS columns. The post-tensioning tendon ratios, ρ = At/Ag (tendon-to-segment area ratio), of 0.005, 0.01, and 0.02 are considered respectively for the 2, 4, and 8-segment columns such that all columns have the same stiffness for the tendon, EtAt/H. Et and At are the elastic modulus and area of the tendon respectively. Constant axial load ratio, N/(fcAg) = 0.2, and initial post-tensioning-to-yield stress ratio, σ0t/σy = 0.4, are selected for the tendon of the columns.

Table 1 – Details of the PPS columns used in this study

Column Label.	n	H (m)	B (m)	ρ	$N/(f_cA_g)$	σ_0^t/σ_y
C2	2	1	0.5	0.005	0.2	0.4
C4	4	2	0.5	0.01	0.2	0.4
C8	8	4	0.5	0.02	0.2	0.4

To simulate nonlinear seismic behaviour of the PPS columns under different ground motions, a 2D Finite Element model made in OpenSees program is used (see Fig. 1). As shown in Fig. 1b, the segments are modelled using Elastic Beam-Column elements. The post-tensioning stainless steel tendon is modelled with a Truss Element. An Elastic Perfectly Plastic material is used to model the tendon. An initial strain was incorporated into the material model to account for the axial shortening due to post-tensioning force of the tendon. The axial load due to the bridge deck was applied as a vertical force on the topmost node of the columns. Furthermore, inertial effects of the bridge deck is considered by applying lumped horizontal and vertical masses to the top node of the columns. These masses are equivalent to the axial force acting on the column. The Lobatto Quadrature integration scheme is employed to distribute the axial stiffness of the segments across the contact surface of individual rocking joints. Each rocking joint/compression zone (see Fig. 2a) is simulated as a series of vertical zero-length gap elements. An elastic zero-tension uniaxial material model is used for the joints to model joint opening and compression forces at the contact surfaces. Further details on the FE model used and its experimental validation are found in [14].

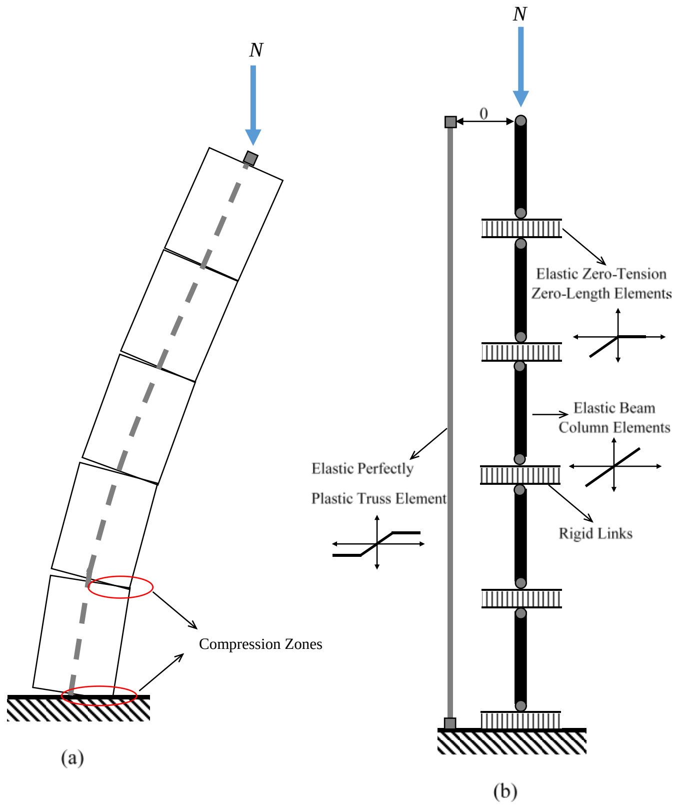

Fig. 1 – 2D FE modelling of PPS columns in OpenSees program

3. Analysis and Results

A set of 44 far-field ground motion records are used for the seismic assessment of the columns. The intensity measure (IM) selected for the IDA analysis in this study is the 5% damped spectral acceleration response at the column's first mode period, Sa (T_1, 5%). T_1 is the first natural vibration period of the column at very low-amplitude dynamic excitations where the joints are still close, and no rocking motion has initiated. Prior to the IDA analysis of each column, the ground motions are first scaled to 1 at the natural period of each column using their 5% damped spectra. The IM is then changed from 0.05g to 1g with the increment of 0.05g. Small IM value of 0.005g very close to 0 is also considered to ensure elastic behavior of the columns before their rocking initiation.

Maximum values of time history responses of the columns for each record and IM value are first determined. Then, the IM values are plotted versus maximum responses to produce IDA curves. The seismic responses considered in this study are top drift, base rotation, base shear, and base moment. Drift response here is defined as the ratio of lateral displacement to column's height; base shear and moment responses are normalised by total weight (W) of the column, and its gravitational moment (BW) respectively.

Fig. 2 shows hysteretic normalised base shear versus top drift of the columns for different values of intensity measures. At IM = 0.005g (Fig. 2a), the columns remain elastic. The column C2 is more stable, and requires higher minimum base excitation to start its rocking motion. Hence, its rocking starts at higher IM values compared to the other columns. Further, as shown in Fig. 2c, the C2 column exhibits a higher energy-dissipation capacity as squat columns are more stable, and have larger contact surfaces.

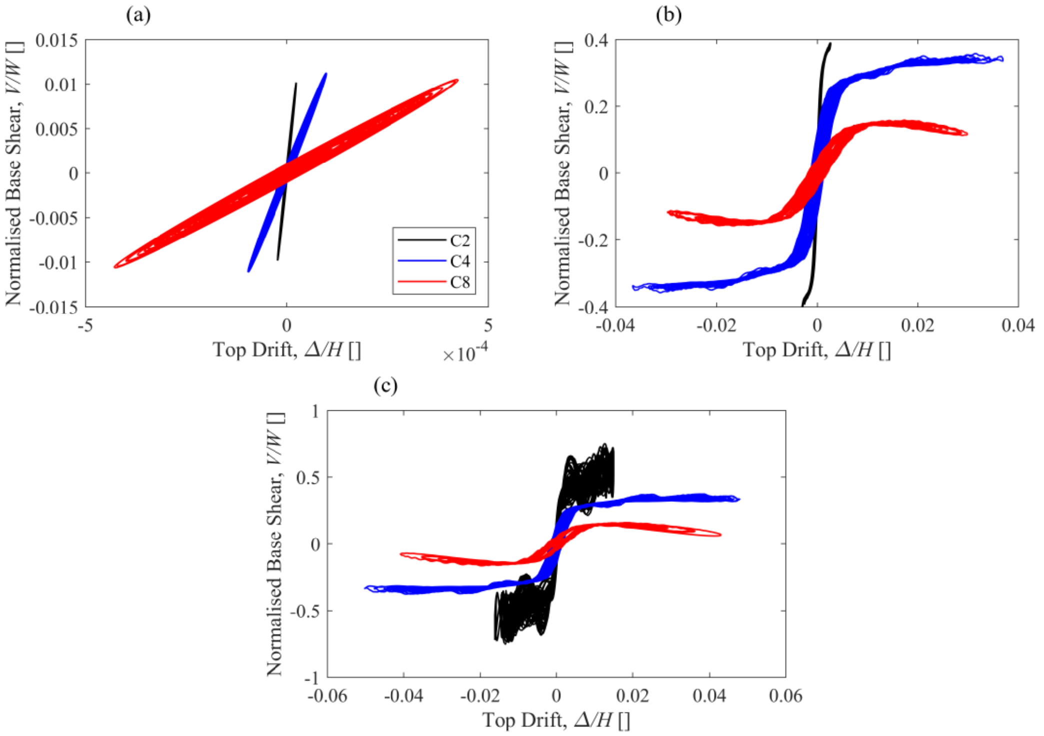

Fig. 2 – Normalised base shear versus top drift of the columns subject to one ground motion: (a) 0.005g, (b) 0.25g, and (c) 0.5g

Fig. 3 compares median IDA curves of all the three columns for various responses. For small IM values, as the column becomes more slender, the top drift becomes larger (see Fig. 3a). The reason lies in the fact that slender columns require smaller minimum ground excitation to start their rocking motion. However, at higher IM values, the squat column gives higher top drift as all the columns have initiated their rocking motion. The median IDA curves of the base rotation exhibit the same trend as the top drift (Fig. 3b). The only difference is the threshold IM value at which the effect of the aspect ratio becomes reversed. The threshold IM value is larger for the top drift. At small IM values, the slope of the median IDA curves for the base shear are very similar as they have similar area of contact at the joints (Fig. 3c). However, the squat column possesses the largest amount of base shear at all IM values. Particularly for the columns C4 and C8, the base shear becomes approximately constant for large IM values as their median IDA curves approach vertical lines. The median IDA curves of the base moment follow a similar trend to the top drift and base rotation. Again, there is a threshold IM value below which the more slender column gives higher base moment. However, above this threshold IM value, the squat column gives larger base moment. Fig. 4 illustrates IDA curves of the column C4 and its median IDA curve for the post-tensioning stress of the tendon normalised by its yielding stress. Fig. 4 compares median IDA curves of the columns for the normalised post-tensioning force of the tendon. The drop in the initial tendon force ratio is due to the prestress loss due to elastic shortening of the segments as well as the flexibility of rocking surfaces under gravity loads. This presstress loss is higher for the more slender columns as they have more number of segments and joints. The post-tensioning force of the tendon is approximately constant for very small IM values (pre-opening phase of the joints), and it increases as the rotation of the joints increases (post-opening phase). Further, the squat column results in a far larger post-tensioning force in the tendon compared to other columns, and the tendon of the squat column, C2, yields at very high IM levels while the other two columns remain elastic.

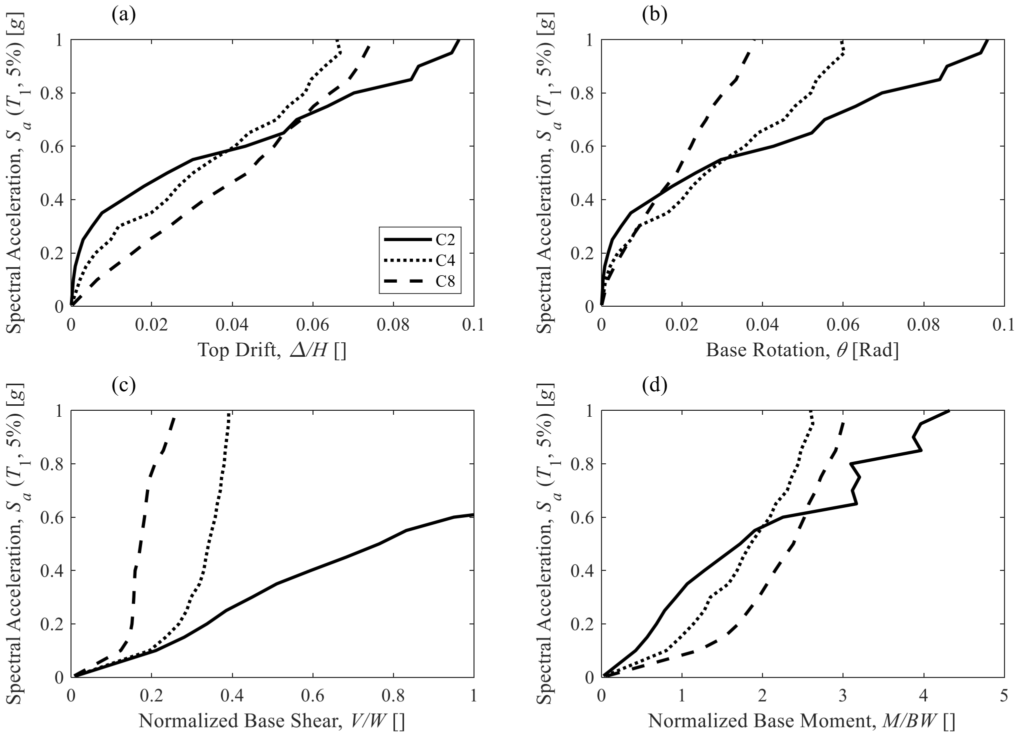

Fig. 3 – Median IDA curves of all ground motions for the columns: (a) top drift, (b) base rotation, (c) normalised base shear, and (d) normalised base moment

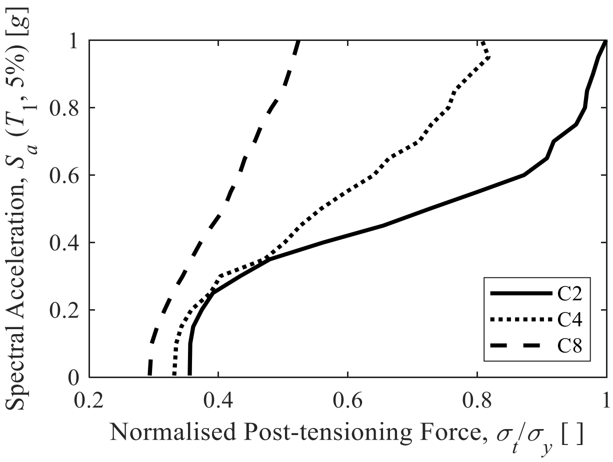

Fig. 4 – Median IDA curves of all ground motions for the normalised post-tensioning force of the columns

Two potential failure can be considered for the PPS columns: (1) as the post-tensioning tendon provides global stability and self-centring capacity of the PPS columns, yielding of the tendon will lead to collapse of such columns, and (2) also, like the CIP columns, extensive strength drop of the PPS columns can happen due to the second order or P-delta effects. Hence, Slight Damage, Moderate Damage, and Extensive Damage states are defined where the tendon stress reaches 0.5σy, 0.7σy, and 0.9σy, respectively. Furthermore, it is assumed that the Extensive Damage begins when the strength loss of the columns reaches 20%. For the column C8, the 20% strength loss occurs far before the yielding of the tendon at small drift values while for the other columns, the yielding of the tendon governs the failure of the column. Fig. 5 illustrates the fragility curves for the columns at different damage states. For the Slight Damage state, the column C2 reaches probability of exceedance 0.9 at IM values of 0.53g while it occurs at IM value of 0.75g for the column C4. In case of Moderate Damage state, probability of exceedance of 0.9 is attained at IM value of 0.68g and 1.1g respectively for the columns C2 and C4. The IM values corresponding to probability of exceedance of 0.9 for the Extensive Damage state are 0.8g and 1.25g respectively for the columns C2 and C4. The slender column, C4, exhibits a better seismic performance compared to the squat column C2. However, the aspect ratio of the column must be limited so that the yielding of the tendon occurs prior to the strength loss of the column.

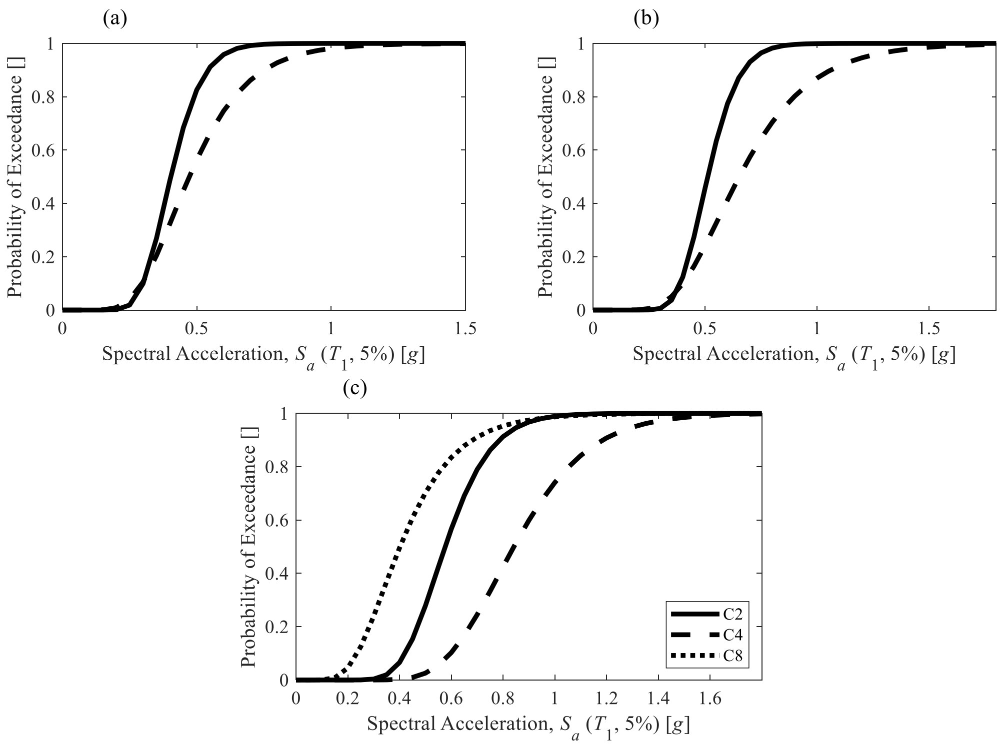

Fig. 5 Fragility curves of the columns C2, C4, and C8: (a) Slight Damage, (b) Moderate Damage, and (c) Extensive Damage

4. Conclusions

In this study, seismic performance of precast post-tensioned segmental columns are assessed through incremental dynamic analysis. An experimentally validated FE model is used to simulate dynamic behavior of three columns with different aspect ratios subject to an extensive ensemble of 44 far-fault ground motions. Median IDA curves curves were then determined to assess seismic behavior of the columns. The IDA curves demonstrated that the maximum drift, relative rotation, shear force, and moment responses occur at the base of the columns, and also, the responses increases as the ground motion intensity increases. It was found from the median IDA curves of the columns that there is a threshold intensity measure below which slenderising the column increases the top drift, base rotation, and base moment. Above this threshold intensity measure, the trend becomes reversed. However, such threshold intensity measure was not seen for the base shear, and the base shear continuously reduced as the column became more slender. It was found that slender columns exhibit fragility curves stretched towards higher intensity measures which demonstrates better seismic performance of slender columns. However, the slenderness of the columns must be capped as the global strength loss might lead to their failure at very small drift values.

5. Acknowledgements

The authors acknowledge the support received by the UK Engineering and Physical Sciences Research Council (EPSRC) for a Prosperous Nation [grant number EP/R039178/1]: SPINE: Resilience-Based Design of Biologically Inspired Columns for Next-Generation Accelerated Bridge Construction].

6. References

[1] Hewes JT (2002): Seismic design and performance of precast concrete segmental bridge columns, PhD Thesis.

[2] Ou YC, Chiewanichakorn M, Aref AJ, Lee GC (2007): Seismic Performance of Segmental Precast Unbonded Posttensioned Concrete Bridge Columns. *Journal of Structural Engineering*, **133** (2007), 1636–1647.

[3] Chou CC, Chen YC (2006): Cyclic tests of post-tensioned precast CFT segmental bridge columns with unbonded strands. *Earthquake Engineering & Structural Dynamics*, **35** (2006), 159–175.

[4] Motaref S, Saiidi M, Sanders D (2010): Experimental Study of Precast Bridge Columns with Built-In Elastomer, Transportation Research Record. *Journal of the Transportation Research Board*, **2202** (2010), 109–116.

[5] Sideris P, Aref AJ, Filiatrault A (2014): Large-Scale Seismic Testing of a Hybrid Sliding-Rocking Posttensioned Segmental Bridge System. *Journal of Structural Engineering*, **140** (2014), 4014-4025.

[6] Kashani MM, Gonzalez-Buelga A (2017): Nonlinear dynamics of self-centring segmental composite rocking column. *Procedia Engineering*, **199** (2017), 441–446.

[7] Kashani MM, Gonzalez-Buelga A, Thayalan RP, Thomas AR, Alexander NA (2018): Experimental investigation of a novel class of self-centring spinal rocking column. *Journal of Sound and Vibration*, **437** (2018). 308–324.

[8] Kashani MM, Ahmadi E, Gonzalez-Buelga A, Zhang D, Scarpa F (2019): Layered composite entangled wire materials blocks as pre-tensioned vertebral rocking columns. *Composite Structures*, **214** (2019), 153–163.

[9] Ahmadi E, Kahshani MM (2019): On the use of entangled wire materials in pre-tensioned rocking columns, *XIIIth International Conference on Recent Advances in Structural Dynamics*, The Institute of Sound and Vibration Research (ISVR), Lyon, France.

[10] Ou YC, Sen Tsai M, Chang KC, Lee GC (2010): Cyclic behavior of precast segmental concrete bridge columns with high performance or conventional steel reinforcing bars as energy dissipation bars. *Earthquake Engineering & Structural Dynamic*s. **39** (2010), 1181–1198.

[11] Motaref S (2011): Seismic Response of Precast Bridge Columns with Energy Dissipating Joints, PhD Thesis.

[12] Zhang N (2014): Dynamic properties and application of steel fiber reinforced self-consolidating concrete to segmental bridge columns in moderate-to-high seismic regions, PhD Thesis.

[13] Cai ZK, Zhou Z, Wang Z (2019): Influencing factors of residual drifts of precast segmental bridge columns with energy dissipation bars. *Advances in Structural Engineering*, **22** (2019), 126–140.

[14] Ahmadi E, Kashani MM (2020): Numerical investigation of nonlinear static and dynamic behaviour of self-centring rocking segmental bridge piers. *Soil Dynamics and Earthquake Engineering*, **128** (2020), 105876.

[15] McKenna F (2011): OpenSees: A framework for earthquake engineering simulation, *Computing in Science and Engineering*, **13** (2011), 58–66.

[16] Vamvatsikos D, Cornell CA (2002): Incremental dynamic analysis. *Earthquake Engineering & Structural Dynamics*, **31** (3), 491-514.

